

This is an Open Access document downloaded from ORCA, Cardiff University's institutional repository:<https://orca.cardiff.ac.uk/id/eprint/84692/>

This is the author's version of a work that was submitted to / accepted for publication.

Citation for final published version:

Morny, Emyan Komla A., Margrain, Tom H. , Binns, Alison M. and Votruba, Marcela 2015. Electrophysiological ON and OFF responses in autosomal dominant optic atrophy. *Investigative Ophthalmology & Visual Science* 56 (13) , pp. 7629-7637. 10.1167/iovs.15-17951

Publishers page: <http://dx.doi.org/10.1167/iovs.15-17951>

Please note:

Changes made as a result of publishing processes such as copy-editing, formatting and page numbers may not be reflected in this version. For the definitive version of this publication, please refer to the published source. You are advised to consult the publisher's version if you wish to cite this paper.

This version is being made available in accordance with publisher policies. See <http://orca.cf.ac.uk/policies.html> for usage policies. Copyright and moral rights for publications made available in ORCA are retained by the copyright holders.



26

27 **Results:** Mean amplitudes of the N95 and all PhNRs, except the full-field PhNR_{ON},
28 were significantly reduced in participants with ADOA ($p < 0.01$). Subtraction of the
29 group averaged focal ERG of ADOA participants from that of controls showed an
30 equal loss in the focal PhNR_{ON} and PhNR_{OFF} components, while in the full-field ERG
31 the loss in the PhNR_{OFF} was greater than that in the PhNR_{ON} component. The Areas
32 Under the ROC Curve (AUC) for the focal PhNR_{ON} (0.92), focal PhNR_{OFF} (0.95) and
33 full-field PhNR_{OFF} (0.83), were not significantly different from that of the PERG N95
34 (0.99).

35

36 **Conclusions:** In patients with ADOA, the PhNR_{ON} and PhNR_{OFF} components are
37 nearly symmetrically reduced in the long duration ERG suggesting that ON- and
38 OFF-RGC pathways may be equally affected.

39 **Introduction**

40 Autosomal dominant optic atrophy (ADOA) is a hereditary optic neuropathy
41 characterized by variable bilateral loss of vision in early childhood, optic nerve pallor,
42 centrocoecal visual field scotoma and color vision defects²⁻⁶. It is the commonest
43 hereditary optic neuropathy with a prevalence between 1 in 50,000 to 1 in 8,000⁷⁻¹².

44

45 ADOA is caused primarily by mutations in the autosomal nuclear gene, *OPA1*^{10, 13-}
46 ¹⁶, a key player in mitochondrial dynamics, controlling mitochondrial fusion, amongst
47 other key roles. Histopathological studies in humans^{17, 18} and mouse models¹⁹⁻²²
48 show that ADOA is principally characterized by the degeneration of the retinal
49 ganglion cells (RGC).

50

51 In a mouse model of ADOA, generated in our laboratory²², the defect is first evident
52 as a dendritic pruning of RGCs in B6:C3-*Opa1*^{Q285STOP} *Opa1* mutant mouse which
53 appears to be ON-center specific^{19, 23}. This selective vulnerability of ON-center
54 RGCs may reflect their higher energy demands in comparison to their OFF-center
55 counterparts, since *OPA1* mutations are thought to curtail mitochondrial energy
56 output^{19, 23}. This new finding has however not been investigated in humans with
57 ADOA.

58

59 The functional integrity of RGCs can be evaluated by assessing the photopic
60 negative response (PhNR) of the flash ERG. The PhNR is a negative potential seen
61 after the b-wave in a photopic ERG elicited by a brief flash. The PhNR is believed to
62 primarily originate from spiking activity in RGCs and their axons with contributions
63 from amacrine cells and possible involvement of associated glial cells/astrocytes of

64 the retina ²⁴⁻²⁷. When a long duration flash is used to evoke the ERG, the PhNR is
65 seen once after the b-wave (PhNR_{ON}) and again as a negative going potential after
66 the d-wave (PhNR_{OFF}). Furthermore, it has been demonstrated that the ERG
67 obtained in response to a long duration red flash of moderate intensity provides
68 optimal delineation of the PhNR_{ON} and PhNR_{OFF} components^{24, 27, 28}.

69

70 The brief flash PhNR is attenuated in patients with ADOA ²⁹ and in the *Opa1*^{Q285STOP}
71 mutant mouse³⁰. In the mouse model, the defect is seen prior to any changes in
72 visual acuity on optokinetic drum testing and prior to morphological changes on
73 retinal histology. This suggests that retinal connectivity may be affected before RGC
74 somal loss impacts on RGC function²³. Thus the PhNR deficit could serve as a
75 marker for early disease. These early changes in RGC function may be reversible
76 and need to be defined as markers for targeted therapies in any forthcoming
77 therapeutic trials.

78

79 Miyata et al (2007) and Barnard et al (2011) highlight the diagnostic potential of the
80 PhNR in ADOA, however, the investigators used a brief white flash (broadband
81 stimulus) to evoke the PhNR, which provides a poor signal to noise ratio compared
82 to monochromatic stimuli²⁷, and cannot distinguish ON and OFF components.
83 Furthermore, the studies elicited full-field (global) PhNRs which, in contrast to the
84 focal PhNR, are less sensitive in detecting focal retinal lesions such as those seen in
85 early to moderate glaucoma ^{31, 32}. As ADOA results in localized centrocoecal visual
86 field defects², it might be expected that a focal stimulus presented to this region
87 would enhance the sensitivity of the PhNR to early disease-related changes.

88

89 The aim of this study was to assess the relative effect of ADOA on the PhNR_{ON} and
90 PhNR_{OFF} components elicited using focal and full-field long duration red flashes on a
91 rod suppressing blue background. An additional aim was to compare the diagnostic
92 potential of the long duration PhNRs to responses which have previously been
93 shown to be affected by ADOA; the full-field brief flash PhNR^{29, 30} and the N95
94 amplitude of the pattern electroretinogram (PERG)³³, which also reflects spiking
95 activity of the RGCs³⁴.

96

97

98 **Methods**

99 ***Participants***

100 Twelve participants (aged 18 – 61 years) from six families with documented *OPA1*
101 mutations and 16 healthy age matched controls (aged 19 – 61 years) were recruited
102 for the study (see Table 1 for characteristics of all 12 participants). Detailed
103 information about the clinical characteristics of nine of the participants have been
104 reported elsewhere². The study conformed to the Declaration of Helsinki and was
105 approved by the National Health Service Research Ethics Committee for Wales as
106 well as the ethics committees of the School of Optometry and Vision Sciences,
107 Cardiff University, and the Division of Optometry and Visual Science, City University,
108 London. All participants provided their written consent after receiving a participant
109 information sheet and having the opportunity to ask questions. Nine participants with
110 ADOA (ID numbers 1010-1017, 1021) were examined in Cardiff and the rest at City
111 University London by the same investigator.

112

113 ***Electroretinograms***

114 All ERGs were recorded monocularly using a DTL fiber active electrode (Unimed
115 Electrode Supplies, Ltd, Surrey, UK) and a contralateral reference. The DTL fiber
116 was placed in the lower fornix to maximize stability during recording and the loose
117 end fastened using medical tape at the inner canthus (Blenderm, Viasys Healthcare
118 Ltd., Warwick, UK). A silver-silver chloride 10mm diameter touch-proof skin electrode
119 (Unimed Electrode Supplies, Ltd, Surrey, UK), placed at the mid-frontal forehead
120 position was used as ground electrode.

121

122 ERG responses were obtained using an evoked potential monitoring system
123 (Medelec EP, Oxford Instruments PLC, Surrey, UK [Cardiff site]; Espion, Diagnosys
124 LLC, Cambridge, UK [City University site]). Responses were bandpass filtered from
125 1 – 100 Hz and digitally averaged. Signals were recorded in blocks of 10 - 20
126 responses, with a total of 40 – 60 averaged per trace. Between 4 and 6 traces were
127 obtained for each stimulus condition. The traces were superimposed to confirm
128 signal repeatability and averaged off-line into a single averaged trace containing 160
129 – 300 responses. An automatic artefact rejection system removed signals
130 contaminated by large eye movements and blinks.

131

132 Transient PERG stimuli (4 reversals per second; check size = 1°) were generated on
133 a computer monitor at 98% contrast. The screen was masked with a black opaque
134 cardboard with a 13 x 13 cm square cut-out at the center so that it produced a 20° x
135 20° field at a viewing distance of 36cm.

136

137 Long duration ERGs were recorded using a red flash stimulus (peak output 660nm,
138 250msec duration, 3.33 log phot td, 2Hz) on a rod saturating blue background (peak

139 output 469nm, 3.49 scot log td) produced by a hand-held miniature Ganzfeld light
140 emitting diode (LED) stimulator (CH Electronics, Kent, UK). Focal stimulation was
141 produced by mounting the miniature Ganzfeld LED tube into the middle of a light box
142 (44 cm x 44 cm x 10 cm) such that the circular stimulus subtended 20° diameter at a
143 viewing distance of 15.6 cm. The 20° stimulus size was chosen to encompass as
144 much of the central field as possible while avoiding the optic disc which starts about
145 12°-15° nasal to the fovea. In order to minimize the effect of stray light stimulating the
146 peripheral retina (i.e. the area outside the stimulus area) the light box contained a
147 strip of white LEDs (Super Bright InGan) passed through a blue filter (Lee Filter 068
148 Sky Blue, Lee Filters, Hampshire, UK) to produce a desensitizing blue surround of
149 3.73 scot log td (field size = 109° x 109° field). Cross hairs centered in the middle of
150 the stimulus served as the fixation target. Full-field ERGs were recorded by holding
151 the stimulator head, fitted with a diffusing cap, directly to the eye.

152

153 Full-field brief (flash) ERGs were elicited by a Ganzfeld stimulator (GS2000, LACE
154 Elettronica, Italy) presenting a xenon flash stimulus (1.76 log td.s, 300 μsec
155 maximum flash duration, 4Hz). Filters were used to obtain a red stimulus (Lee Filter
156 “Terry Red”, Lee Filters, Hampshire, UK, transmittance <5% at wavelengths shorter
157 than 575 nm, and above 85% from 625–700 nm) over a continuous rod saturating
158 3.39 scot log td blue background (Schott Glass filter BG28, Schott AG, Mainz,
159 Germany, peak transmittance 454 nm). All stimulus backgrounds were of sufficient
160 scotopic illuminance to saturate the rods³⁵.

161

162 All ERGs were recorded by the same investigator using the same protocol at both
163 sites. Long duration ERGs (focal and full-field) were generated by the same

164 miniature Ganzfeld LED stimulator at both sites. PERG and full-field brief flash data
165 were only obtained from participants attending Cardiff University, in order to ensure
166 consistency. All stimuli were calibrated using an ILT 1700 radiometer with
167 SED033/Y/R luminance detector (Able Instruments and Controls, Reading, UK)
168 assuming a 7 mm pupil with no correction for the Stiles-Crawford effect. The
169 wavelength of the light sources were measured using a Specbos 1201 spectro-
170 radiometer (Horiba Jobin Yvon Ltd, Middlesex, UK).

171

172 ***Procedures***

173 All participants underwent a comprehensive ophthalmic examination which included
174 best corrected visual acuity (ETDRS), contrast sensitivity (Pelli-Robson), visual field
175 assessment (24-2 SITA-FAST, Humphrey Visual Field Analyzer), slit lamp
176 biomicroscopy, optical coherence tomography (OCT; Topcon 3D-OCT 1000), fundus
177 photography, color vision (D-15 desaturated test) and auto-refraction. In order to
178 target earlier stage ADOA, the eye with the better visual field mean deviation score
179 was selected for ERG recording, with the dominant eye chosen in the case of equal
180 scores between the two eyes.

181

182 PERGs were always recorded first with natural pupils and near refractive correction
183 when necessary. Pupils were then dilated using 1% tropicamide to a minimum of
184 7mm and flash ERGs were recorded in the following order: focal long-duration, full-
185 field long duration and full-field brief flash ERG.

186

187 ***Signal Analysis***

188 PERGs and focal ERGs were Fourier analyzed to remove high frequency noise
189 above 30Hz and 50Hz respectively. The method for measuring the amplitude of the
190 various sub-components is described in Figure 1. The PhNR_{ON} (PhNR for brief flash
191 ERG) and PhNR_{OFF} amplitudes were measured from the pre-stimulus baseline and
192 voltage at stimulus offset respectively to a fixed time point in their respective troughs.
193 When determining the most appropriate fixed time point at which to measure the
194 PhNR_{ON} and PhNR_{OFF} responses, the group averaged ERG of ADOA participants
195 was subtracted from the group averaged ERG of the controls to obtain a difference
196 ERG. The implicit time of the greatest discrepancy between the two was identified for
197 the PhNR_{ON} and PhNR_{OFF} responses and was used as the fixed time point for all
198 measurements. The fixed times at which the PhNR amplitudes were measured were
199 as follows: focal PhNR_{ON} at 95 msec after onset, focal PhNR_{OFF} at 97 msec after
200 offset, full-field PhNR_{ON} at 83 msec after onset, full-field PhNR_{OFF} at 102 msec after
201 offset and full-field brief PhNR at 72 msec after onset. The identification of all peaks
202 and troughs was determined objectively using Microsoft Excel i.e. as the
203 minimum/maximum voltage within a fixed time window.

204

205 ***Statistical Analysis***

206 Data expressed on a logarithmic scale (i.e. visual acuity, contrast sensitivity and
207 visual field mean deviation) were converted (anti-logged) into a linear scale to
208 calculate mean and standard deviation (SD) values. The mean and SD values were
209 then converted back to log units. The distribution of the ERG data was checked for
210 normality using the Shapiro-Wilk test. Where data were normally distributed,
211 independent samples t-tests (2-tailed) were used to compare controls and
212 participants with ADOA; the Mann-Whitney U test was used where data were non-

213 normally distributed. In order to minimize Type 1 errors due to the number of
214 comparisons made ($n = 35$), we applied a Bonferroni adjustment to the alpha level
215 (0.05) and report observations as significant when $p \leq 0.0014$. Receiver Operating
216 Characteristic (ROC) curve analysis was used to calculate the area under the curve
217 (AUC) to assess the diagnostic potential of the various ERG components. The
218 comparison between AUCs were made using the method described by Hanley and
219 McNeil (1983)³⁶.

220

221

222 **Results**

223 The clinical characteristics of all 12 ADOA participants from 6 families are shown in
224 Table 1. The means and standard deviation for visual acuity, contrast sensitivity and
225 mean deviation were 1.10 ± 1.07 logMAR, 1.30 ± 1.26 log units and -7.39 ± 7.09 dB
226 respectively. The visual field defects were mostly central or centrocecal and color
227 vision defects were variable but participants from the same family had similar
228 defects. More details regarding the relationship between the clinical characteristics
229 and ERG data in ADOA participants is to be the subject of a future manuscript.

230

231 ***Pattern ERGs***

232 PERGs recorded from 9 ADOA participants are shown superimposed on the group
233 averaged trace of 16 controls in the left hand column of Figure 2A. It shows that the
234 negative N95 component is reduced in amplitude for all participants with ADOA,
235 beyond the 95% confidence intervals for the control data. The P50 amplitudes in
236 ADOA participants were also below the lower 95% confidence intervals except for
237 one participant. The middle column of Figure 2A and the data in Table 2

238 demonstrate that the mean P50 and N95 amplitudes were significantly reduced in
239 ADOA participants compared to controls. The mean N95:P50 ratio in ADOA
240 participants of 1.05 was significantly reduced compared to 1.73 in controls (Table 2).
241 Although there was evidence of P50 and N95 loss in people with ADOA, the
242 difference plot in the right hand column of Figure 2A is dominated by a negative
243 going signal corresponding to the loss of the N95 component.

244

245 ***Focal Long Duration Cone ERGs***

246 Focal long duration cone ERGs recorded from 12 participants with ADOA are shown
247 superimposed on the group averaged trace of 16 controls in the left column of Figure
248 2B. The typical ERG responses were characterized by the a-wave, b-wave, PhNR_{ON},
249 d-wave and PhNR_{OFF}. The PhNR_{ON} was reduced in amplitude below the lower 95%
250 confidence limit of the control data in almost all ADOA participants except one.
251 Notably, the waveform after stimulus offset varied considerably between ADOA
252 participants. For instance in participants with ADOA, the most prominent positive
253 peak after stimulus offset, assumed to be the d-wave, was delayed and had a broad
254 peak whose maximum amplitude occurred at highly variable times (Figure 2B, right
255 and middle columns). In comparison, this prominent peak was highly consistent
256 between control participants with respect to implicit time and was reflected in the
257 much smaller standard deviation of the d-wave implicit time in controls than in
258 participants with ADOA (Table 2).

259

260 The difference plot (Figure 2B, right) was dominated by two negative going waves
261 representing the PhNR_{ON} and PhNR_{OFF} components affected by ADOA. The

262 difference plots of the ON and OFF components had similar profiles and amplitudes
263 2.80 μV and 2.88 μV respectively.

264

265 ***Long Duration Full-field Cone ERG***

266 The long duration full-field cone ERGs in Figure 2C were recorded from the same
267 ADOA participants (thin lines) and controls (group averaged thick black line) as the
268 focal cone ERGs in Figure 2B. The form of the long duration ERG was similar under
269 focal and full-field conditions with one exception. There were two positive peaks
270 immediately after light offset in the full-field ERG; the first being the d-wave^{24, 37}. The
271 mean amplitude of the PhNR_{OFF}, but not the PhNR_{ON}, was significantly reduced in
272 participants with ADOA (Table 2). On the difference plot (Figure 2C, right) the
273 amplitude of the PhNR_{OFF} difference (8.76 μV) was more than twice the amplitude of
274 the PhNR_{ON} difference (3.42 μV) when measured.

275

276 Once again, the OFF components showed greater variability than ON components
277 for participants with ADOA. In fact, in at least 6 participants with ADOA, there was a
278 third positive peak (3PP) after light offset not seen in controls (Figure 2C, left). There
279 was no obvious pattern to the presence or absence of the 3PP in ADOA participants.

280 The amplitude and implicit time of the 3PP measured from the ADOA group
281 averaged trace was 13.34 μV and 75 msec after light offset respectively.

282 Comparatively, none of the control traces displayed the 3PP prominently, although
283 on close visual inspection, a kink corresponding in time with the 3PP was observed
284 in some individual control traces.

285

286 ***Comparison of Focal and Full-field Long Duration ERGs***

287 The waveform of the focal and full-field long duration ERGs was further compared by
288 normalizing the group averaged ERGs to their respective b-wave amplitudes (Figure
289 3). The focal and full-field ERGs of controls (Figure 3A) and participants with ADOA
290 (Figure 3B) had similar profiles although implicit times of the b-wave, PhNR_{ON} and d-
291 wave were significantly delayed in the focal ERG ($p \leq 0.01$, data not shown). The
292 most prominent positive peak of the focal ERG after light offset coincided with the
293 2PP of the full-field ERG in the control traces while in the ADOA group, the broad
294 peak of the focal ERG after offset described a curve that roughly matched the profile
295 of the 2PP and 3PP of the full-field ERG.

296

297 In controls, the PhNRs are proportionally greater in the focal ERG than in the full-
298 field ERG (Figure 3A). The losses in amplitudes of the PhNRs were also greater in
299 the focal ERG than the full-field ERG in participants with ADOA (Figure 3B and 3C).

300

301 ***The Brief Full-field ERG***

302 Brief full-field ERG recorded from 7 ADOA participants are shown in Figure 2D.
303 Typical ERG responses had a-wave, b-wave, i-wave and PhNR components. The
304 PhNR amplitude was reduced significantly in people with ADOA compared to
305 controls (Figure 2D and Table 2). The difference plot in the right hand column of
306 Figure 2D indicates that the greatest deficit in ADOA corresponds to the timing of the
307 b-wave and the PhNR. An i-wave was recorded for all participants (controls and
308 ADOA). Although it appeared more prominent in ADOA participants, there was no
309 statistical difference in amplitude or implicit time between control and ADOA
310 participants (Table 2).

311

312 ***Specificity and Sensitivity of the Different ERGs***

313 Receiver operating characteristics (ROC) curves were used to determine the
314 effectiveness of the N95 and long duration focal and full-field PhNRs at
315 discriminating participants with ADOA from controls for 9 participants with ADOA and
316 16 controls for whom PERG and long duration focal and full-field ERG data were
317 available (Figure 4). The AUC, sensitivity, specificity and cut off value which
318 produced an optimal sensitivity while maintaining minimum specificity of ~90% are
319 shown in Table 3. The N95 amplitude had the greatest diagnostic power. However, a
320 comparison of the AUCs of the focal and full field PhNRs with the N95 amplitude,
321 using the method described by Hanley and McNeil (1983)³⁶ showed that the N95
322 amplitude was only significantly more sensitive than the full-field PhNR_{ON} amplitude
323 ($z = 2.12$). Therefore, considered in terms of their diagnostic ability, the focal PhNRs
324 and N95 component were not significantly different.

325

326

327 **Discussion**

328 ***Effect of ADOA on ON and OFF Retinal Ganglion Cells***

329 In this study we sought to determine whether the PhNR_{ON} was preferentially affected
330 in ADOA as might be predicted based on the study by William et al¹⁹. Our findings
331 however showed that in human patients, the PhNR_{ON} and PhNR_{OFF} amplitudes were
332 equally reduced in the focal ERG, while in the full-field ERG, there was a greater
333 reduction in the PhNR_{OFF} amplitude than the PhNR_{ON} amplitude. What then might
334 explain this apparent contradiction?

335

336 In the study by William et al (2010), evidence for the preferential loss of ON-RGCs
337 was based on mouse retinal flat mounts showing significant dendritic pruning of ON-
338 but not OFF-RGCs. The experiment reported here however assessed the effect of
339 ADOA on the ON- and OFF-RGCs by evaluating the PhNR amplitude of the human
340 ERG, a functional measure. The role of the RGCs as primary originators of the
341 PhNR has been demonstrated by Frishman and colleagues^{24-27, 34}. In experiments
342 using long duration full-field ERGs, they showed that that PhNR_{ON} and PhNR_{OFF}
343 components were both reduced or eliminated after experimental glaucoma and
344 intravitreal injection of tetrodotoxin (TTX) (an agent that blocks generation of sodium
345 dependent spikes in retinal neurons) in macaque, as well as in patients with
346 glaucoma. Although, the origins of the PhNR_{ON} and PhNR_{OFF} have not been
347 conclusively traced to the ON- and OFF-RGCs respectively, Luo and Frishman³⁴
348 showed that the PhNR_{ON} (and b-wave) component but not the PhNR_{OFF} (or d-wave)
349 was eliminated after injecting 2-amino-4-phosphonobutyric acid (APB) into the
350 macaque retina to block synaptic transmission from photoreceptors to ON-bipolar
351 cells and hence ON-RGCs. Injecting TTX after APB then removed the PhNR_{OFF} but
352 not the d-wave thereby linking the PhNR_{ON} and PhNR_{OFF} components (although
353 indirectly) to the ON and OFF pathways respectively.

354

355 Previous human^{31, 38, 39} and animal^{24, 30} studies (including our mouse model) have
356 shown that the PhNR amplitude is very susceptible to RGC damage with severe
357 attenuation of PhNR amplitude recorded even when morphologic and other
358 functional parameters were within normal range i.e. in early stage disease. It is
359 possible that the PhNR_{ON} pathways may be selectively compromised at an earlier
360 stage of the disease process than that studied here. A similar study in pre-

361 symptomatic people with the *OPA1* mutations or in people with ADOA at a much
362 earlier stage of the disease (e.g. children with ADOA) could provide additional
363 insights.

364

365 Our findings may also be a reflection of the heterogeneous nature of ADOA. There
366 are over 200 *OPA1* mutations^{15, 16} which cause ADOA with wide phenotypic
367 variations both within and between affected families^{2, 40}. Genotype-phenotype
368 correlations have been difficult to establish in previous studies^{3, 41} and the number of
369 patients in each family of *OPA1* mutations (except Family E) was insufficient to
370 reliably explore such correlations. In the mouse model, the mutant mice (>10 months
371 old) were genetically homogenous and disease severity correlated with age.
372 Participants studied here were from 6 families, with a different mutation in each
373 family (Table 1), and at different stages of the disease. This may have diluted
374 observations that would have been made from a homogenous cohort.

375

376 ***Comparison of Focal and Full-field PhNRs***

377 The long duration focal and full-field ERGs in this study were recorded using the
378 same stimulus parameters, which were comparable to the parameters recommended
379 by Kondo et al⁴² for eliciting focal responses. Although the waveforms of the focal
380 and full field ERGs were similar, they were not identical (Figure 3A-B). There was a
381 greater contribution of PhNR_{ON} and PhNR_{OFF} components to the focal ERG than to
382 the full-field ERG (Figure 3A) which reflects the decreasing proportion of RGCs to
383 other retinal cells with eccentricity⁴³. The focal PhNRs were more severely affected
384 than their full-field counterparts by ADOA and this was reflected in the larger AUCs
385 found for the focal signals. These findings were consistent with the central field

386 defects recorded in ADOA participants in this study and in others^{2, 6, 44}. In addition,
387 whereas the focal PhNRs were both significantly reduced ($p < 0.001$), only the full-
388 field PhNR_{OFF} was significantly reduced in the full-field ERG (Table 2). Although the
389 N95 and focal PhNR amplitudes were highly discriminatory for ADOA, it should be
390 noted that the participants in this study had relatively late stage disease.

391

392 The symmetrical loss in the focal PhNR_{ON} and PhNR_{OFF} amplitudes (Figure 2B right
393 column and Figure 3C) may reflect the 1:1 ratio of ON- to OFF-RGCs in the macula,
394 while the greater loss in the full-field PhNR_{OFF} amplitude than the PhNR_{ON} amplitude
395 (Figure 2C right column and Figure 3C) may reflect the nearly 1:2 ratio of ON- to
396 OFF-RGCs in the peripheral retina⁴⁵⁻⁴⁷. The broadening of the d-wave peak in the
397 focal ERG and the presence of the 3PP in the full-field long ERG in participants with
398 ADOA may be due to contributions from the cone receptor potential (CRP) and/or
399 depolarizing OFF-bipolar cell responses after light offset which were unmasked in
400 the relative absence of the negative going PhNR_{OFF}⁴⁸⁻⁵⁰. The 2PP may be the i_{OFF}-
401 wave described by Horn et al (2011)⁵¹, although in contrast to their results, this study
402 did not record a significant difference in amplitude between controls and participants
403 with ADOA.

404

405 ***Comparison to other Electrophysiological Studies in ADOA***

406 Miyata et al²⁹ reported a significant reduction in the full-field brief PhNR, but none in
407 the a- or b-wave amplitude, in ADOA patients using white-on-white stimulus. Similar
408 results were obtained by Barnard et al³⁰ in the mouse model. In this present study,
409 we show similar results using a red on blue stimulus. The flash luminance used in
410 this study was adopted from a previous study in this laboratory⁵² and was

411 comparable to the flash luminance used by Miyata et al²⁹. This supports findings that
412 the red-on blue stimulus is effective for clinical evaluation of RGC function.

413

414 Holder et al³³ reported a significant reduction in N95 amplitude and the N95:P50 ratio
415 of the PERG participants with ADOA. We obtained similar results and showed that
416 the focal PhNRs and N95 amplitude were equally effective at discriminating controls
417 from participants with ADOA. The focal ERG could therefore be used as an
418 alternative to the PERG.

419

420 In this study, as well as in that of Holder et al³³, the P50 amplitude was significantly
421 reduced. This may indicate that bipolar cell function is compromised in ADOA as has
422 been put forward by Reis et al⁵³. However, a reduction in P50 amplitude is also seen
423 when only RGCs are compromised³⁴, therefore the P50 reduction observed in this
424 study could be due to dysfunction of bipolar cells, RGCs or both.

425

426 **Conclusion**

427 This study showed there was a nearly symmetrical reduction in the PhNR_{ON} and
428 PhNR_{OFF} amplitudes in participants with ADOA with no evidence of a preferential
429 ON-pathway loss. This suggests that ON- and OFF-RGCs may be equally affected in
430 patients. In addition, in terms of their diagnostic potential, the focal PhNR-ON and -
431 OFF amplitudes were better than their full-field counterparts and were not
432 significantly different from the N95 amplitude of the PERG.

433

434 **Acknowledgement**

435 EM is funded by the Ghana Education Trust Fund. We acknowledge Fight for Sight
436 Small Grants Award (MV), for their contribution to genotyping.

437 **REFERENCES**

- 438 1. Marmor MF, Brigell MG, McCulloch DL, Westall CA, Bach M. ISCEV standard
439 for clinical electro-oculography (2010 update). *Documenta Ophthalmologica*
440 2011;122:1-7.
- 441 2. Votruba M, Fitzke FW, Holder GE, Carter A, Bhattacharya SS, Moore AT.
442 Clinical features in affected individuals from 21 pedigrees with dominant optic
443 atrophy. *Arch Ophthalmol* 1998;116:351-358.
- 444 3. Votruba M, Thiselton D, Bhattacharya SS. Optic disc morphology of patients
445 with OPA1 autosomal dominant optic atrophy. *Br J Ophthalmol* 2003;87:48-53.
- 446 4. Newman NJ, Biousse V. Hereditary optic neuropathies. *Eye* 2004;18:1144-
447 1160.
- 448 5. Yu-Wai-Man P, Griffiths PG, Hudson G, Chinnery PF. Inherited mitochondrial
449 optic neuropathies. *J Med Genet* 2009;46:145-158.
- 450 6. Votruba M, Moore AT, Bhattacharya SS. Clinical features, molecular genetics,
451 and pathophysiology of dominant optic atrophy. *J Med Genet* 1998;35:793-800.
- 452 7. Krill AE, Smith VC, Pokorny J. Similarities between congenital tritan defects
453 and dominant optic-nerve atrophy - coincidence or identity *J Opt Soc Am*
454 1970;60:1132-&.
- 455 8. Kjer B, Eiberg H, Kjer P, Rosenberg T. Dominant optic atrophy mapped to
456 chromosome 3q region .2. Clinical and epidemiological aspects. *Acta Ophthalmol*
457 *Scand* 1996;74:3-7.
- 458 9. Votruba M, Aijaz S, Moore AT. A review of primary hereditary optic
459 neuropathies. *J Inherit Metab Dis* 2003;26:209-227.
- 460 10. Yu-Wai-Man P, Griffiths PG, Burke A, et al. The prevalence and natural
461 history of dominant optic atrophy due to OPA1 mutations. *Ophthalmology*
462 2010;117:1538-1546, 1546.e1531.
- 463 11. Gallus GN, Cardaioli E, Rufa A, et al. High frequency of OPA1 mutations
464 causing high ADOA prevalence in south-eastern Sicily, Italy. *Clin Genet*
465 2012;82:277-282.
- 466 12. Lenaers G, Hamel C, Delettre C, et al. Dominant optic atrophy. *Orphanet J*
467 *Rare Dis* 2012;7.
- 468 13. Alexander C, Votruba M, Pesch UEA, et al. OPA1, encoding a dynamin-
469 related GTPase, is mutated in autosomal dominant optic atrophy linked to
470 chromosome 3q28. *Nat Genet* 2000;26:211-215.
- 471 14. Delettre C, Lenaers G, Griffoin JM, et al. Nuclear gene OPA1, encoding a
472 mitochondrial dynamin-related protein, is mutated in dominant optic atrophy. *Nat*
473 *Genet* 2000;26:207-210.
- 474 15. Ferre M, Bonneau D, Milea D, et al. Molecular Screening of 980 Cases of
475 Suspected Hereditary Optic Neuropathy with a Report on 77 Novel OPA1 Mutations.
476 *Hum Mutat* 2009;30:E692-E705.
- 477 16. Ferre M, Amati-Bonneau P, Tourmen Y, Malthiery Y, Reynier P. eOPA1: An
478 online database for OPA1 mutations. *Hum Mutat* 2005;25:423-428.
- 479 17. Johnston PB, Gaster RN, Smith VC, Tripathi RC. A clinicopathologic study of
480 autosomal dominant optic atrophy. *Am J Ophthalmol* 1979;88:868-875.
- 481 18. Kjer P, Jensen OA, Klinken L. Histopathology of eye, optic-nerve and brain in
482 a case of dominant optic atrophy. *Acta Ophthalmol (Copenh)* 1983;61:300-312.
- 483 19. Williams PA, Morgan JE, Votruba M. Opa1 deficiency in a mouse model of
484 dominant optic atrophy leads to retinal ganglion cell dendropathy. *Brain*
485 2010;133:2942-2951.

- 486 20. Sarzi E, Angebault C, Seveno M, et al. The human OPA1delTTAG mutation
487 induces premature age-related systemic neurodegeneration in mouse. *Brain*
488 2012;135:3599-3613.
- 489 21. Alavi MV, Bette S, Schimpf S, et al. A splice site mutation in the murine Opal
490 gene features pathology of autosomal dominant optic atrophy. *Brain* 2007;130:1029-
491 1042.
- 492 22. Davies VJ, Hollins AJ, Piechota MJ, et al. Opa1 deficiency in a mouse model
493 of autosomal dominant optic atrophy impairs mitochondrial morphology, optic nerve
494 structure and visual function. *Hum Mol Genet* 2007;16:1307-1318.
- 495 23. Williams PA, Piechota M, von Ruhland C, Taylor E, Morgan JE, Votruba M.
496 Opa1 is essential for retinal ganglion cell synaptic architecture and connectivity.
497 *Brain* 2012;135:493-505.
- 498 24. Viswanathan S, Frishman LJ, Robson JG, Harwerth RS, Smith EL, 3rd. The
499 photopic negative response of the macaque electroretinogram: reduction by
500 experimental glaucoma. *Invest Ophthalmol Vis Sci* 1999;40:1124-1136.
- 501 25. Viswanathan S, Frishman LJ, Robson JG. The uniform field and pattern ERG
502 in macaques with experimental glaucoma: removal of spiking activity. *Invest*
503 *Ophthalmol Vis Sci* 2000;41:2797-2810.
- 504 26. Viswanathan S, Frishman LJ, Robson JG, Walters JW. The photopic negative
505 response of the flash electroretinogram in primary open angle glaucoma. *Invest*
506 *Ophthalmol Vis Sci* 2001;42:514-522.
- 507 27. Rangaswamy NV, Shirato S, Kaneko M, Digby BI, Robson JG, Frishman LJ.
508 Effects of Spectral Characteristics of Ganzfeld Stimuli on the Photopic Negative
509 Response (PhNR) of the ERG. *Invest Ophthalmol Vis Sci*. United States; 2007:4818-
510 4828.
- 511 28. Sustar M, Hawlina M, Brecelj J. ON- and OFF-response of the photopic
512 electroretinogram in relation to stimulus characteristics. *Doc Ophthalmol*
513 2006;113:43-52.
- 514 29. Miyata K, Nakamura M, Kondo M, et al. Reduction of oscillatory potentials and
515 photopic negative response in patients with autosomal dominant optic atrophy with
516 OPA1 mutations. *Invest Ophthalmol Vis Sci* 2007;48:820-824.
- 517 30. Barnard AR, Issa PC, Perganta G, et al. Specific deficits in visual
518 electrophysiology in a mouse model of dominant optic atrophy. *Exp Eye Res*
519 2011;93:771-777.
- 520 31. Machida S, Tamada K, Oikawa T, et al. Comparison of photopic negative
521 response of full-field and focal electroretinograms in detecting glaucomatous eyes.
522 *Journal of ophthalmology* 2011;2011.
- 523 32. Tamada K, Machida S, Yokoyama D, Kurosaka D. Photopic negative
524 response of full-field and focal macular electroretinograms in patients with optic
525 nerve atrophy. *Jpn J Ophthalmol* 2009;53:608-614.
- 526 33. Holder GE, Votruba M, Carter AC, Bhattacharya SS, Fitzke FW, Moore AT.
527 Electrophysiological findings in dominant optic atrophy (DOA) linking to the OPA1
528 locus on chromosome 3q 28-qter. *Doc Ophthalmol* 1998;95:217-228.
- 529 34. Luo X, Frishman LJ. Retinal Pathway Origins of the Pattern Electroretinogram
530 (PERG). *Invest Ophthalmol Vis Sci* 2011;52:8571-8584.
- 531 35. Aguilar M, Stiles WS. Saturation of the rod mechanism of the retina at high
532 levels of stimulation. *Opt Acta (Lond)* 1954;1:59-65.
- 533 36. Hanley JA, McNeil BJ. A method of comparing the areas under receiver
534 operating characteristic curves derived from the same cases. *Radiology*
535 1983;148:839-843.

- 536 37. Evers HU, Gouras P. Three cone mechanisms in the primate
537 electroretinogram: two with, one without off-center bipolar responses. *Vision Res*
538 1986;26:245-254.
- 539 38. Nakamura H, Miyamoto K, Yokota S, Ogino K, Yoshimura N. Focal macular
540 photopic negative response in patients with optic neuritis. *Eye (Lond)* 2011;358-364.
- 541 39. Gotoh Y, Machida S, Tazawa Y. Selective loss of the photopic negative
542 response in patients with optic nerve atrophy. *Arch Ophthalmol* 2004;341-346.
- 543 40. Granse L, Bergstrand I, Thiselton D, et al. Electrophysiology and ocular blood
544 flow in a family with dominant optic nerve atrophy and a mutation in the OPA1 gene.
545 *Ophthalmic Genet* 2003;24:233-245.
- 546 41. Yu-Wai-Man P, Griffiths PG, Gorman GS, et al. Multi-system neurological
547 disease is common in patients with OPA1 mutations. *Brain* 2010;133:771-786.
- 548 42. Kondo M, Kurimoto Y, Sakai T, et al. Recording focal macular photopic
549 negative response (PhNR) from monkeys. *Invest Ophthalmol Vis Sci* 2008;3544-
550 3550.
- 551 43. Curcio CA, Allen KA. Topography of ganglion-cells in human retina. *J Comp*
552 *Neurol* 1990;300:5-25.
- 553 44. Fuhrmann N, Schimpf S, Kamenisch Y, et al. Solving a 50 year mystery of a
554 missing OPA1 mutation: more insights from the first family diagnosed with autosomal
555 dominant optic atrophy. *Mol Neurodegener* 2010;5.
- 556 45. Dacey DM, Petersen MR. Dendritic field size and morphology of midget and
557 parasol ganglion-cells of the human retina. *Proc Natl Acad Sci U S A* 1992;89:9666-
558 9670.
- 559 46. Dacey DM. The mosaic of midget ganglion cells in the human retina. *J*
560 *Neurosci* 1993;13:5334-5355.
- 561 47. Drasdo N, Millican CL, Katholi CR, Curcio CA. The length of Henle fibers in
562 the human retina and a model of ganglion receptive field density in the visual field.
563 *Vision Res* 2007;47:2901-2911.
- 564 48. Bush RA, Sieving PA. A proximal retinal component in the primate photopic
565 ERG a-wave. *Invest Ophthalmol Vis Sci* 1994;35:635-645.
- 566 49. Ueno S, Kondo M, Ueno M, Miyata K, Terasaki H, Miyake Y. Contribution of
567 retinal neurons to d-wave of primate photopic electroretinograms. *Vision Res*
568 2006;46:658-664.
- 569 50. Sieving PA, Murayama K, Naarendorp F. Push-pull model of the primate
570 photopic electroretinogram: a role for hyperpolarizing neurons in shaping the b-wave.
571 *Vis Neurosci* 1994;11:519-532.
- 572 51. Horn FK, Gottschalk K, Mardin CY, Pageni G, Junemann AG, Kremers J. On
573 and off responses of the photopic fullfield ERG in normal subjects and glaucoma
574 patients. *Doc Ophthalmol* 2011;122:53-62.
- 575 52. Mortlock KE, Binns AM, Aldebasi YH, North RV. Inter-subject, inter-ocular and
576 inter-session repeatability of the photopic negative response of the electroretinogram
577 recorded using DTL and skin electrodes. *Doc Ophthalmol* 2010;121:123-134.
- 578 53. Reis A, Mateus C, Viegas T, et al. Physiological evidence for impairment in
579 autosomal dominant optic atrophy at the pre-ganglion level. *Graefes Arch Clin Exp*
580 *Ophthalmol* 2013;251:221-234.
- 581
582

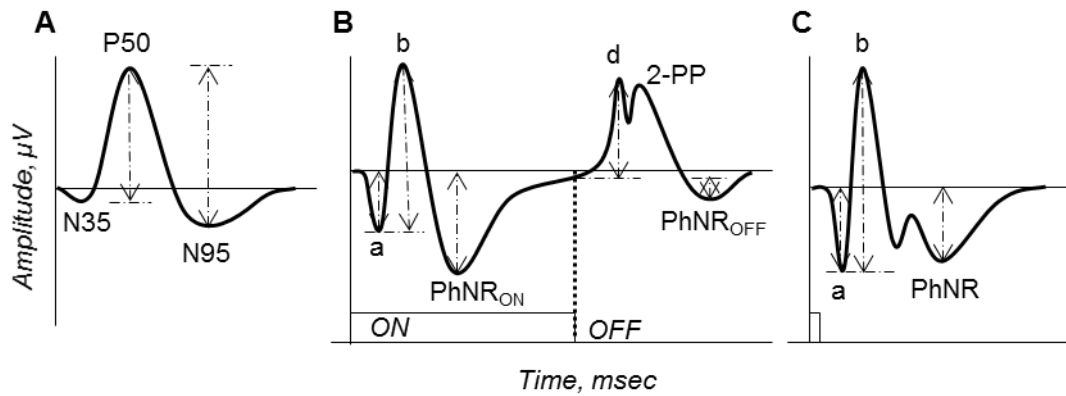


Figure 1. Representative ERG traces of the (A) PERG, (B) full-field long-duration ERG and (C) full-field brief flash ERG showing their components and how their amplitudes were measured (double headed arrows). The amplitudes of the P50, N95 (A), a-wave (a) and b-wave (b) (B-C) were measured as recommended by the International Society of Clinical Electrophysiology of Vision (ISCEV)¹. The d-wave (d) amplitude was measured from the point of light offset to the peak of the d-wave. The PhNR_{ON} (PhNR in brief flash) and PhNR_{OFF} amplitudes were measured from the pre-stimulus baseline and voltage at stimulus offset respectively to a fixed time point in their respective troughs (see main text for details). The focal long duration ERG had the same profile as the full-field long duration except that in the focal ERG there was only one prominent positive peak after light offset, the d-wave.

584

585

586 Table 1. Clinical Characteristics of Participants with ADOA

Participant ID/Gender	Family	Age	Visual Acuity, logMAR		Contrast Sensitivity, log units		Mean Deviation, dB		Color Vision	OPA1 Mutation
			RE	LE	RE	LE	RE	LE		
1010/F	A	49	1.34	1.32	0.35	0.40	-27.03	-25.15	Mixed	c.1202G>A
1011/F	B	55	1.64	1.62	0.00	0.00	-17.65	-19.58	Mixed	C1508A
1012/F	C	58	0.80	1.00	1.15	1.05	-8.68	-10.39	Mixed	IVS8+5G>A
1013/F	C	61	1.10	0.64	NA	NA	-12.47	-9.06	Mixed	IVS8+5G>A
1014/M	D	33	1.40	1.32	0.30	0.45	-13.84	-11.89	Protan/Deutan	NA
1015/F	D	31	1.02	0.98	1.05	1.05	-13.98	-13.20	Protan/Deutan	NA
1016/F	E	18	0.80	0.80	1.65	1.35	-7.08	-8.15	Tritan	IVS9+3A>T
1017/F	E	27	0.82	0.80	1.65	1.65	-5.14	-5.82	Tritan	IVS9+3A>T
1018/F	E	59	0.86	0.96	0.90	0.75	-9.55	-7.03	Tritan	IVS9+3A>T
1019/F	E	49	0.72	1.20	1.50	1.50	-5.99	-6.79	Tritan	IVS9+3A>T
1020/M	E	46	0.98	1.20	1.65	1.20	-10.15	-8.21	Tritan	IVS9+3A>T
1021/M	F	39	0.02	0.00	1.65	1.65	-1.31	-2.25	NA	c.357delT

587 NA – Not available

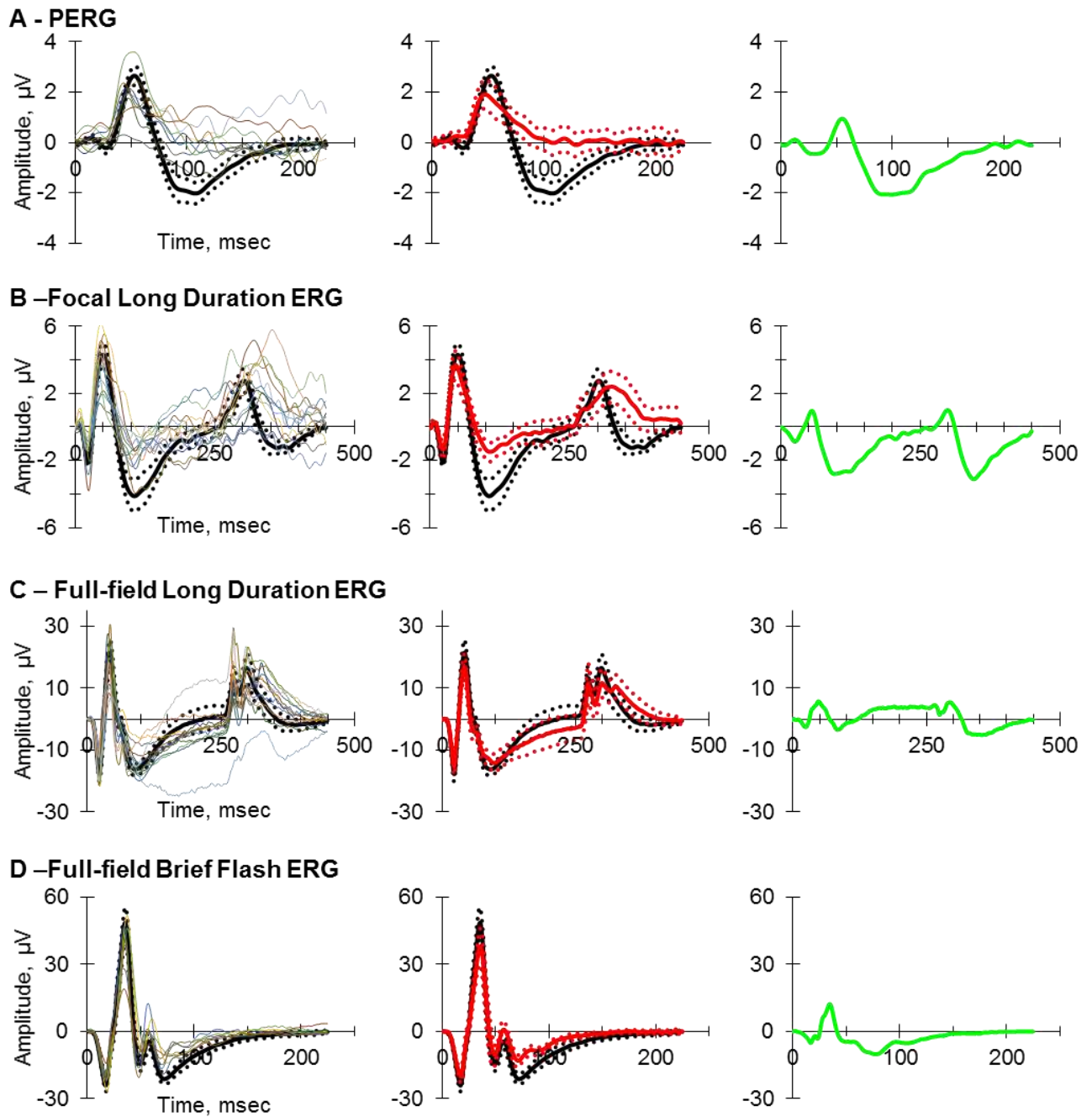


Figure 2. ERG traces of the (A) PERG, (B) focal long duration ERG, (C) full-field long duration ERG and (D) full-field brief flash ERG recorded from participants in this study. Left column: individual traces of participants with ADOA (thin lines) superimposed on the group averaged ERG of 16 controls (thick lines) for each type of ERG recorded. The number of participants with ADOA in A, B, C and D are 9, 12, 12 and 7 respectively. Dotted lines represent 95% confidence intervals. Middle column: comparison between group-averaged traces of controls (thick black line) and ADOA participants (thick red line). Right column: difference plots generated by subtracting the group-averaged ADOA ERG from the control ERG.

590 Table 2. Means of Amplitudes and Implicit Times in Controls and Participants with ADOA

ERG TYPE	Component		ADOA Mean Values	Control Mean Values	P-value
PERG	P50	A, μ V	1.92 \pm 0.81	3.18 \pm 0.81	0.0011*
		T, msec	49.03 \pm 3.67	53.16 \pm 3.28	0.0082
	N95	A, μ V	2.12 \pm 1.31	5.20 \pm 0.87	0.0000*
		T, msec	101.67 \pm 11.21	99.77 \pm 7.76	0.6212 [†]
	N95:P50 Ratio		1.05 \pm 0.31	1.73 \pm 0.47	0.0009* [†]
Focal ERG	a-wave	A, μ V	1.76 \pm 0.94	2.22 \pm 0.61	0.1301
		T, msec	23.00 \pm 1.72	23.75 \pm 1.74	0.2534
	b-wave	A, μ V	5.29 \pm 2.08	6.76 \pm 1.74	0.0524
		T, msec	46.25 \pm 3.14	49.81 \pm 4.88	0.0271
	PhNR _{ON}	A, μ V	1.02 \pm 0.97	3.81 \pm 1.74	0.0000*
		T, msec	109.25 \pm 7.16	104.50 \pm 8.49	0.1299
	d-wave	A, μ V	2.81 \pm 1.52	3.12 \pm 1.04	0.5290
		T, msec	321.92 \pm 13.80	302.41 \pm 5.92	0.0004*
	PhNR _{OFF}	A, μ V	-1.97 \pm 1.52	0.93 \pm 1.23	0.0000*
		T, msec	138.08 \pm 9.94	113.09 \pm 14.64	0.0000* [†]
Full-field Long ERG	a-wave	A, μ V	15.87 \pm 4.44	18.84 \pm 4.45	0.0917
		T, msec	22.50 \pm 1.09	23.16 \pm 1.70	0.2537
	b-wave	A, μ V	33.57 \pm 10.67	41.29 \pm 11.18	0.0768
		T, msec	41.83 \pm 2.86	42.16 \pm 2.47	0.7515
	PhNR _{ON}	A, μ V	12.26 \pm 3.95	15.68 \pm 4.36	0.0430
		T, msec	96.18 \pm 9.16	92.72 \pm 4.15	0.2471
	d-wave	A, μ V	15.11 \pm 6.20	12.84 \pm 4.89	0.2866
		T, msec	274.67 \pm 1.15	273.47 \pm 1.02	0.0075 [†]
	2 nd positive peak	A, μ V	15.48 \pm 4.87	16.10 \pm 7.55	0.8064
		T, msec	302.50 \pm 8.35	298.19 \pm 2.00	0.1054 [†]
PhNR _{OFF}	A, μ V	-8.31 \pm 5.69	0.45 \pm 5.74	0.0005*	
	T, msec	178.33 \pm 27.02	132.19 \pm 17.30	0.0000* [†]	
Full-field Brief ERG	a-wave	A, μ V	20.60 \pm 3.79	25.73 \pm 5.91	0.0480 [†]
		T, msec	17.50 \pm 0.69	17.22 \pm 0.76	0.4133
	b-wave	A, μ V	59.75 \pm 14.58	77.88 \pm 18.17	0.0302
		T, msec	35.39 \pm 1.51	35.38 \pm 1.26	0.9767
	i-wave	A, μ V	14.00 \pm 8.37	16.19 \pm 7.58	0.5420
		T, msec	58.04 \pm 2.04	57.61 \pm 2.37	0.6844
PhNR	A, μ V	12.93 \pm 3.38	22.39 \pm 6.17	0.0011*	
	T, msec	72.75 \pm 4.13	70.59 \pm 6.40	0.4244 [†]	

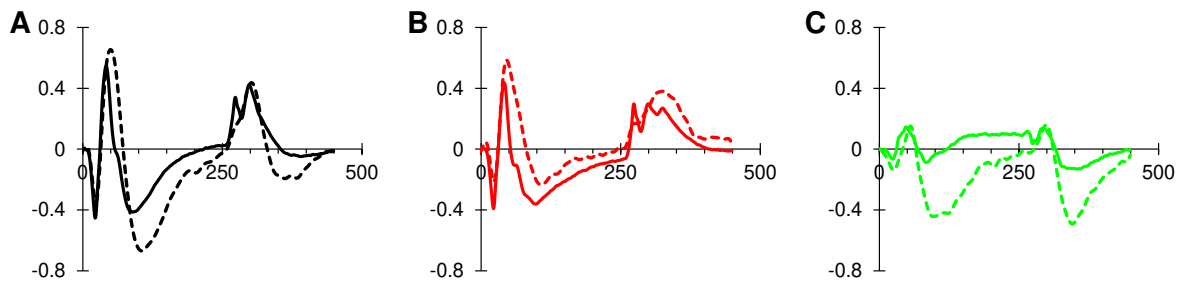
591 Data are expressed as mean \pm standard deviation.

592 A – Amplitude; T – Implicit time from stimulus onset

593 * – Value is significant at $p \leq 0.0014$ level; [†] – data was non-uniformly distributed and Mann-Whitney
 594 U test was used for statistical comparison.

595

596



597

598 Figure 3. A comparison of the long duration focal (dashed lines) and full field (solid lines) group-
 599 averaged ERGs for (A) controls, (B) participants with ADOA and (C) difference plots. ERGs have
 600 been normalised to the b-wave amplitude of their respective control group-averaged ERG.

601

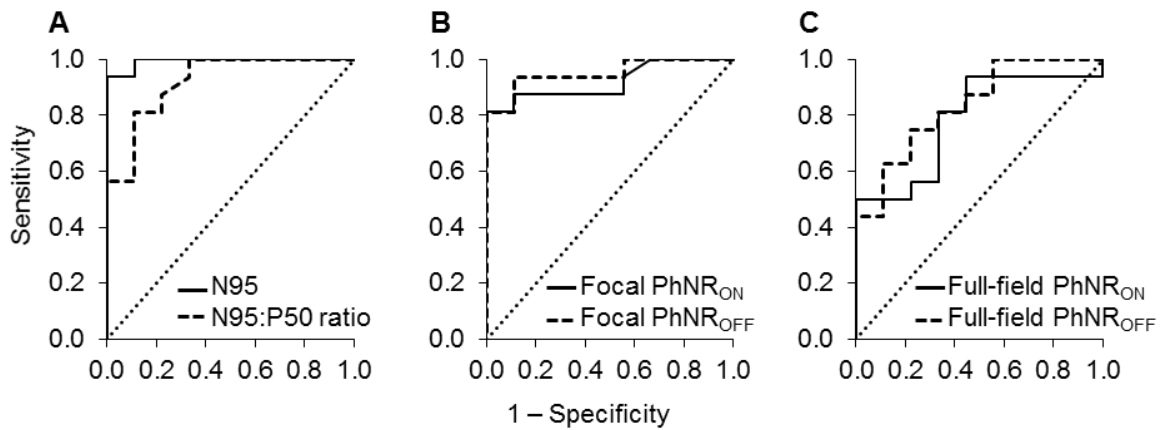


Figure 4. Receiver Operating Characteristic (ROC) curves derived using (A) N95 component and N95:P50 ratio of the PERG, (B) focal PhNR_{ON} and PhNR_{OFF} amplitudes and (C) full-field PhNR_{ON} and PhNR_{OFF} amplitudes. Diagonal dashed line is the reference line.

602

603

604

605 Table 3. Sensitivity, Specificity and Area Under Curve of ROC Analysis for ERG Components

Test Variable	Area (95% CI)	Sensitivity	Specificity	Cut Off Value
N95	0.99 (0.97 – 1.00)	93.80	100.00	4.12 μ V
N95:P50	0.92 (0.81 – 1.00)	81.30	89.90	1.44
Focal PhNR _{ON}	0.92 (0.81 – 1.00)	81.30	100.00	2.62 μ V
Focal PhNR _{OFF}	0.95 (0.87 – 1.00)	81.30	100.00	0.24 μ V
Full-field PhNR _{ON}	0.78 (0.60 – 0.97)	50.00	100.00	16.99 μ V
Full-field PhNR _{OFF}	0.83 (0.73 – 0.99)	62.50	89.90	0.35 μ V

606